Materials Research Proceedings 41 (2024) 763-770 https://doi.org/10.21741/9781644903131-84

Behavior of volumetric core defects in friction extrusion of wire from Al-Cu alloy

RATH Lars[1,a *], SUHUDDIN Uceu F. H.[1,b] and KLUSEMANN Benjamin[1,2,c]

[1]Helmholtz-Zentrum Hereon, Institute of Materials Mechanics, Solid State Materials Processing, Max-Planck Straße 1, 21502 Geesthacht, Germany

[2]Leuphana University Lüneburg, Institute of Product and Process Innovation, Universitätsallee 1, 21335 Lüneburg, Germany

[a]lars.rath@hereon.de, [b]uceu.suhuddin@hereon.de, [c]benjamin.klusemann@hereon.de

Keywords: Friction Extrusion, Solid-State Processing, Aluminum-Copper

Abstract. Friction extrusion describes the processing of metallic materials by inducing severe plastic deformation via frictional heating and shear strain. Rotational motion between die and feedstock is the key feature defining the potential of the process to generate consolidated extrudates with refined, homogenized microstructure. In this study, the effect of volumetric core defects on the material flow and properties of the extrudate is investigated, by processing from Al-Cu billets with a centric bore. Optical as well as scanning electron microscopy, X-ray microtomography and micro-hardness measurements are applied. Different material flow patterns and defect closure mechanisms are identified in correlation with the defect volume and the potential of controlling material flow via geometrical feedstock modification is discussed.

Introduction

First patented in 1993 by Thomas et al. [1], friction extrusion is characterized as the forming of metals under pressure and shear deformation. The basic principle involves the exertion of axial force by a die unto contained feedstock. Applied differential rotation between die and container results in frictional heating and shear introduction into the material, which consequently plasticizes and is being extruded, undergoing severe plastic deformation. The benefits of the process include improved energy efficiency compared to conventional extrusion and suitability for recycling purposes by using chips as feedstock, as systematically investigated by Baffari et al. [2]. The imposed material deformation furthermore can lead to significant microstructural changes with benefits for mechanical or chemical application, mainly based on the effective consolidation, refinement and homogenization of the material.

Friction extrusion of wires from machining chips of Al-Cu alloys has been investigated by Tang and Reynolds [3], observing an equiaxed and recrystallized microstructure with homogeneous ductility and hardness. Typical defects occurring on the wire surface were suggested to be in correlation with the extrusion temperature, setting the processing limits. Hosseini et al [4] performed closer investigation of the bonding between chips of AA 2025, identifying an influence of process parameters on void or defect behavior. Insufficient bonding between AlCu10 chips during friction extrusion was also reported in dependency from the extrusion ratio by Rath et al. [5] as a result of local pressure and thermal conditions in front of the die. Friction extrusion of square bars from scrap AA 1050 by Gelaw et al. [6], and the recycling of AA 7277 to produce wire via friction-stir extrusion by Behnagh et al. [7] further demonstrate the potential of this solid-state process. Due to largely different behavior of aluminum alloy groups in terms of e.g. oxide formation, warm strength, plasticizing behavior and phase formation related effects, transfer of results has to be considered carefully.

Approaches to build a general understanding of the underlying mechanism in friction extrusion have been made. Li et al. [8] applied a marker-insert-technique to visualize material flow, showing a severe influence of changing thermal and shear conditions over process time on the homogenization in the extrudate. Zhao et al. [9] employed digital image correlation to derive an experimentally validated model using viscous fluids. By correlating strain and texture with local conditions during friction extrusion, another advance was made by Li et al. [10] in 2016.

The identified objective for this study therefore is to gain further inside on the material flow and its interaction with volumetric defects as typically occurring in feedstock from chips. Further interest lies in investigating a potential technical solution to control this material flow and enhance defect closure during processing. In rotation-symmetrical wire or bar extrusions, the shear introduction to the core of the billet is severely hindered by the distance to the die face and generally deteriorating shearing conditions as investigated by Halak et al. [11]. The result is a core area with low grain refinement and, in case of chips reduced defect elimination, whereas the outer regions of the wire take full benefit from the high deformation introduced [12].

Typical conditions, which help to reduce core inhomogeneity, are often not applicable as they involve a high extrusion ratio, the use of fine powder feedstock [13] or necessitate strict control of the time and temperature variable shearing conditions in front of the die [11]. Consequently, this work investigates the deformation mechanisms and microstructural changes in the core region by means of analyzing introduced defects throughout processing.

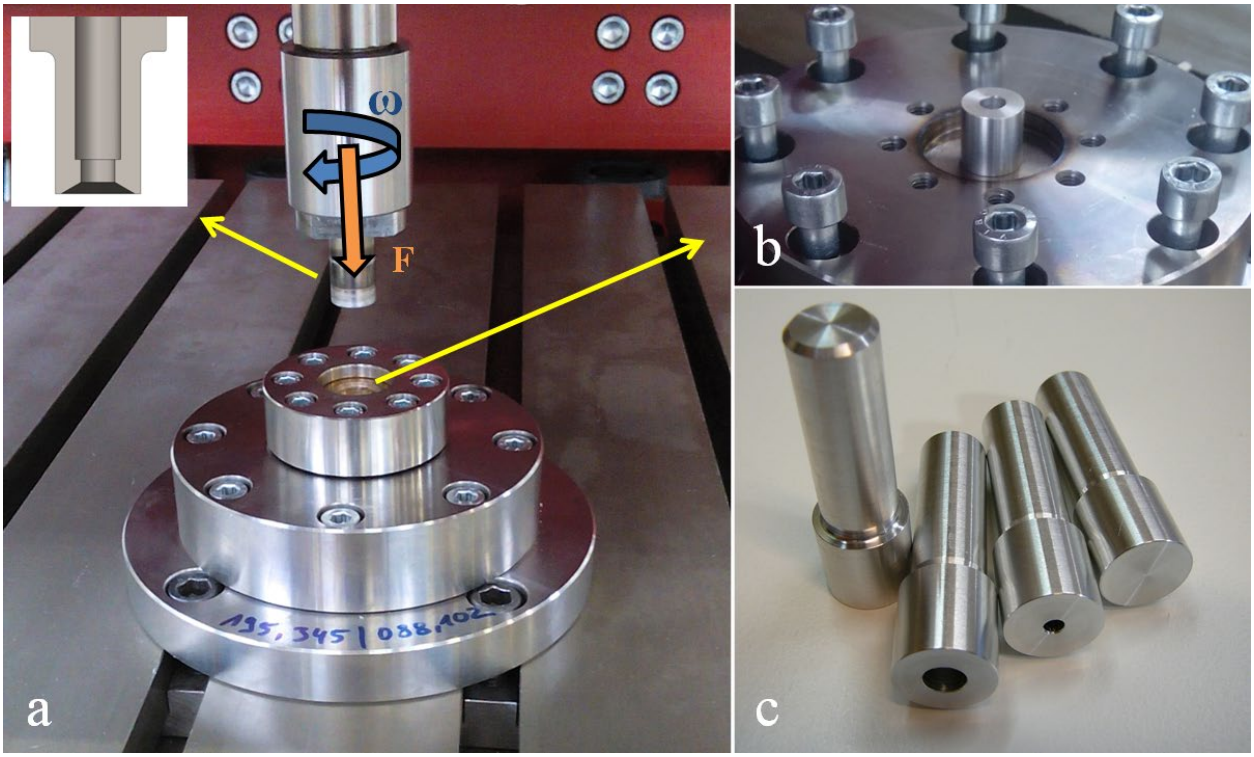

Fig. 1: a) Vertical friction extrusion setup with rotating die, b) AA 2219 billet clamped to the backing and c) billets with 6 and 3 mm centric bore as well as solid feedstock.

Experimental Methods

Feedstock Material. A wrought aluminum-copper alloy, AA 2219, suitable for structural components due to its high fracture toughness and resistance to stress corrosion cracking is used in this study. Billets of 15 mm diameter with 15 mm length plus a 12 mm diameter clamping section, see Fig. 1c, are machined from AA 2219 bar material in solution heat-treated, cold worked and artificially aged T8511 temper. Some of the billets are modified by introducing centric bores of 3 and 6 mm. The depth of the bore amounts to 10 mm plus a 118° drill tip angle.

Friction Extrusion Processing. The friction extrusion of 6 mm wires is performed on a vertical spindle friction surfacing system, Henry Loitz Robotik. The billets are clamped to a steel backing, see Fig. 1b, in order to lock rotation and a hollow cylinder from gunmetal CC493K is clamped to the backing acting as a container for the feedstock material, while providing low friction in contact with the die. The rotating die plunging into the contained billet, see Fig. 1a, has a 120° opening angle with a featureless face, a 6 mm die orifice and a 4 mm bearing length. The die and the container setup are from 42CrMo4+QT steel. For the extrusions, the die is advanced in force control at 14 kN while rotating at 1000 rpm. No pre-heating step or ramping is applied and the extrusion is stopped by die retraction under rotation at a targeted 7 mm plunge depth. At least two processes for each billet geometry were performed under identical processing conditions.

Analysis. For assessment of processing behavior, the machine feedback is recorded: axial force and rotational speed as control as well as spindle torque and die displacement as response parameters. The extruded wires are scanned in X-ray microtomography, Y.Cougar SMT from Xylon International, to detect void volume and progression of the introduced core defect. Scan settings of 115 kV and 60 µA were found to yield optimal contrast for defect detection. Further investigation of the extrudates involves the metallographic preparation by grinding to grit size 4000 with SiC-foil and subsequent polishing with 1 µm diamond suspension. Electrolytic etching was applied with Barker's reagent for 90 s at 15 V. Optical microscopy is performed with a VHX-6000 digital microscopy from Keyence. Hereby, the transitions zone from feedstock to extrudate is of particular interest. For scanning electron microscopy a Quanta 650, FEI Company, field emission gun is used with focus on the immediate grain structure and topology of the defect closure area. Additionally, microhardness of cross-sections along the extrudate as well as over the processing zone are analyzed. Therefore, Vickers indentation maps (HV 0.2, 0.3 mm x 0.3 mm grid) are measured on a Durascan G5, Struers, after allowing for at least 60 days of natural aging.

Results and Discussion

Processing Behavior. While both the billets with and without introduced bore are processed with same control parameters, the void volume or the bore effectively lowers the extrusion ratio (ER). Depending on the individual material flow behavior, the resulting ER, relevant for estimating local pressure and strain conditions, lies between 6.25 and the respectively lower values given in Table 1. This value is not necessarily constant over the process time, but gives a first explanation for the observed change in average plunge speed during the extrusion phase, Fig. 2, ranging from 0.4 mm/s for the solid billets to 0.5 mm/s for billets with 6 mm bore.

Another factor affecting the process response besides the change in feedstock volume lies in the change of extrusion resistance. This shows as a combined effect of the die angle and the removed core material, facilitating radial material flow towards the introduced void volume. However, when looking at the actual axial force as well as the torque feedback, the extrusion resistance is still depending on material flow, as shown by the inverse effect of bore diameter on axial force and torque for 3 and 6 mm bores, Table 1.

A different pressure distribution across the die face is a possible explanation, although the axial force feedback has to be considered carefully, since in force-control mode an offset to the set value (14 kN) indicates accelerations or vibrations exceeding the capability of the employed controller.

Table 1: Average process response parameters for each billet geometry during steady die plunge phase in force-controlled friction extrusion as well as the nominal extrusion ratio.

	Avg. axial force [kN]	Avg. torque [Nm]	Avg. plunge speed [mm/s]	Nominal extrusion ratio
Solid billet	13.0	40.9	0.407	6.25
3 mm bore	13.1	36.8	0.440	6.00
6 mm bore	12.3	39.8	0.500	5.25

The die advance over plunge time presents a nearly constant progression, see Fig. 2, after the initial plunge. In this 1-1.5 s phase the 120° conical inflow region of the die is filled with material and near-constant pressure conditions are established. A slight acceleration over process time in the following extrusion phase is observed for all processes and indicates an overall rising processing temperature. All processes resulted in virtually solid wires with 5.8-5.9 mm outer diameter and a length of 30-40 mm.

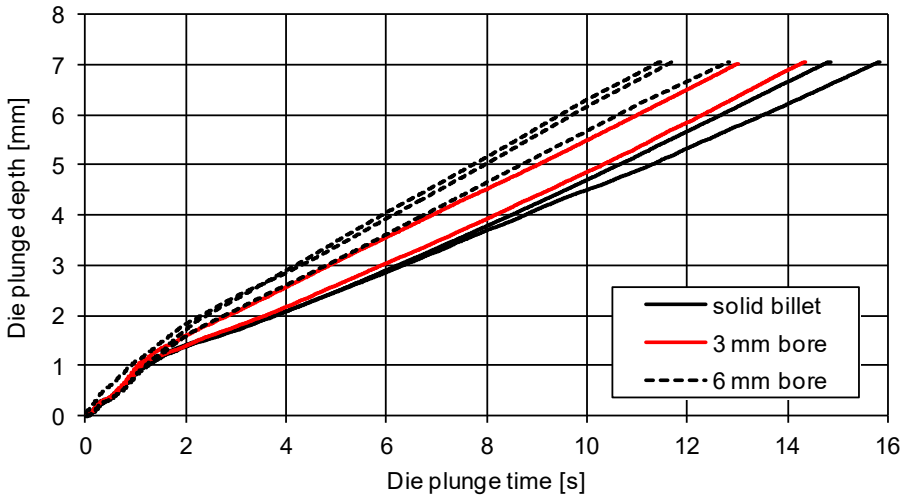

Fig. 2: Die plunge depth over time for the extrusion phase in friction extrusions from solid billets as well as billets with 3 and 6 mm centric bore. Identical process control parameters applied.

Core Defect Analysis. The X-ray microtomography revealed a significant difference in distance from the wire tip for which a volumetric defect could be detected. A direct comparison of 3D-scans from representative samples of all processed billet geometries is shown in Fig. 3a. Here the length difference of the extruded wires as a result of the altered feedstock volume is clearly visible, as well as the remainders of the introduced bores in the feedstock as well as the core defects present in the wire tips.

Upon closer inspection of the wire tips, Fig. 3b, a defect length of 10-15 mm and 3-4 mm for wires from billets with 3 and 6 mm bore, respectively, is measured in the central longitudinal plane of the wires. Due to a resolution limit of approximately 50 µm, the actual defect length is potentially longer. Removing more of the billet's core material not only facilitated radial material flow in combination with the die angle as confirmed by process response parameters, but also removed the material that typically undergoes lower shear deformation or simply elongation, as discussed by Halak et al. [03]. This material would be expected to exert higher resistance to deformation and its removal leaves feedstock with larger but in process less persistent defects. The removal of the feedstock material that typically shows low grain refinement during extrusion by dynamic recrystallization leaves a more or less thick-walled tube-like core structure with higher resistance to radial compression. This model could explain the higher persistence of the core defect in billets with initially lower defect volume.

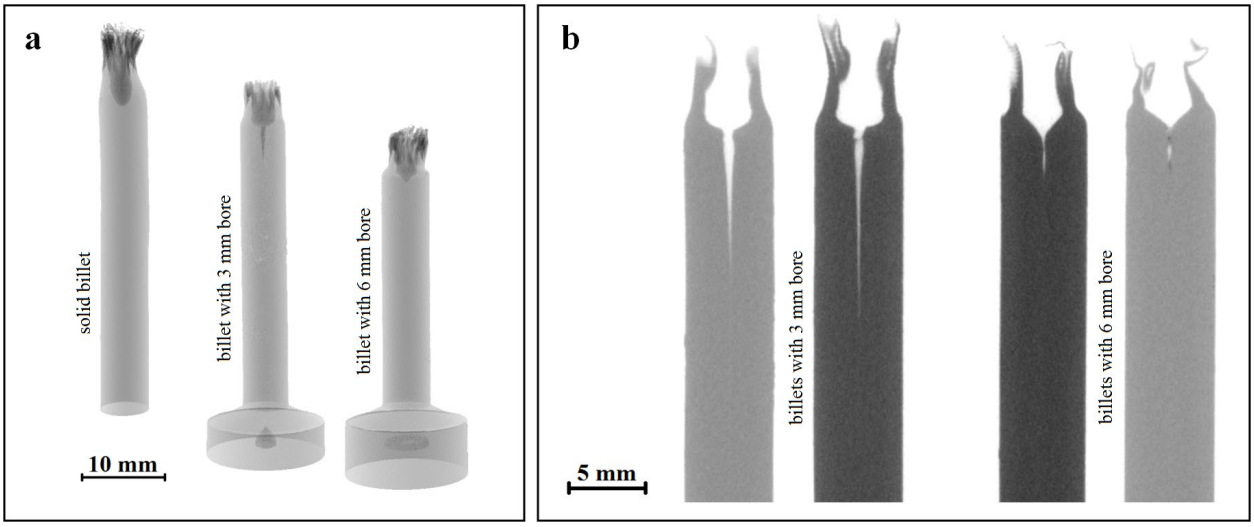

Fig. 3: X-ray microtomography for detection of void volume: a) 3D- scans of wires and residual feedstock friction extruded from different billet geometry and b) central longitudinal plane through wire tips showing closure of the introduced core defects.

Microstructure Analysis. Metallographic analysis of the transition zone from feedstock to wire allowed for more information about the material flow to be obtained. All samples show a highly comparable material flow at the die-feedstock interface, where grain refinement is induced, shaping the outer shell of the extruded wire. The shear-affected zones reaching from the die face into the billets have a similar geometry.

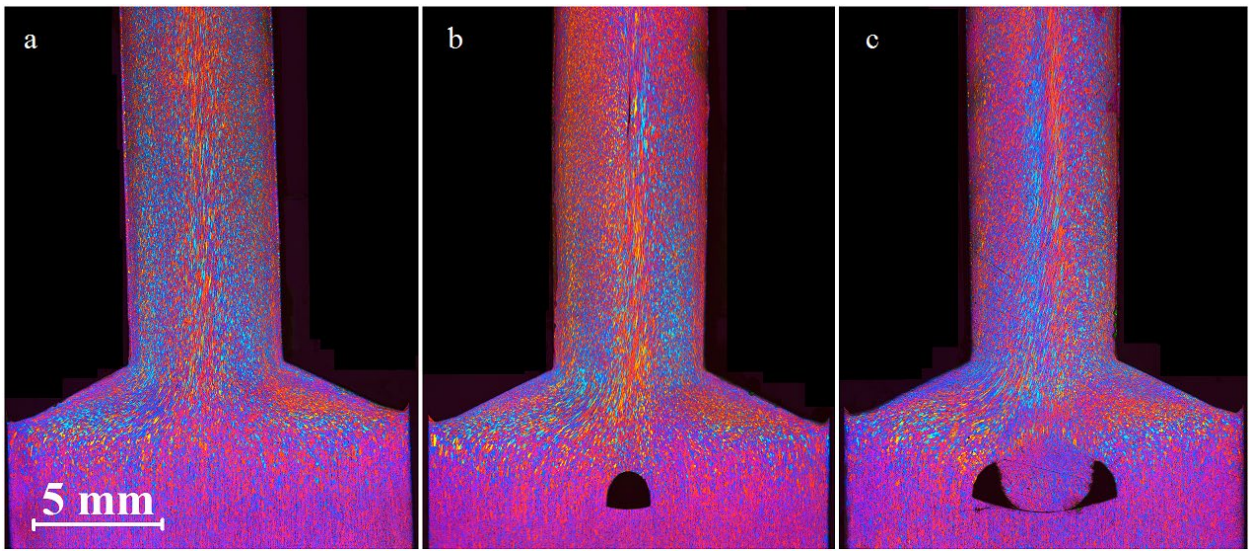

Fig. 4: Optical microscopy: Etched cross-sections of the feedstock-wire transition zone for friction extrusion processes from a) solid billet, b) billets with 3 mm and c) 6 mm bore.

In the billets with 3 mm bore, Fig. 3b, the material flow is closing just before significant microstructural changes are introduced, bypassing or going around the defect without large impact on the process zone. In contrast, in billets with 6 mm bore, Fig. 3c, a flow of refined material away from the die into the introduced defect is observed. The material flow pattern around the defect joins in this case closer to the die orifice in a region where high deformation and partial recrystallization is already present. This difference conforms to the observed force and torque response, Table 1, and shows in the core structure of the wires as well: While in the first case (3 mm bore) a macrograph similar to extrusion from a solid billet is obtained, in the latter case

(6 mm bore) a split in grain orientation is observed in the wire core. Despite this, the grain elongation and torsion around the extrusion axis are comparable.

Scanning Electron Microscopy. The tip of the defect in wire extruded from a billet with 3 mm bore is shown in Fig. 5. The elongated grain structure observed before in the wire core, Fig. 4, is visible here by alignment of precipitates. The grains are radially compressed towards the defect without noticeable deflection from the extrusion axis. In direct proximity to the crack tip, intergranular cracks appear to occur. The defect closure mechanism in this case can be clearly differentiated from the backflow phenomena observed in billets with 6 mm bore, as only radial compression and simultaneous elongation are present, further explaining the longer presence of the defect. This gradually reduces in diameter with increasing processing temperature and decreasing material resistance. It should be noted, that the actual defect tip is difficult to analyze, due to mismatch in imaging plane and angle with the defect or wire axis. The possible continuous presence of a core defect in the wires extruded from 3 mm billets cannot be excluded.

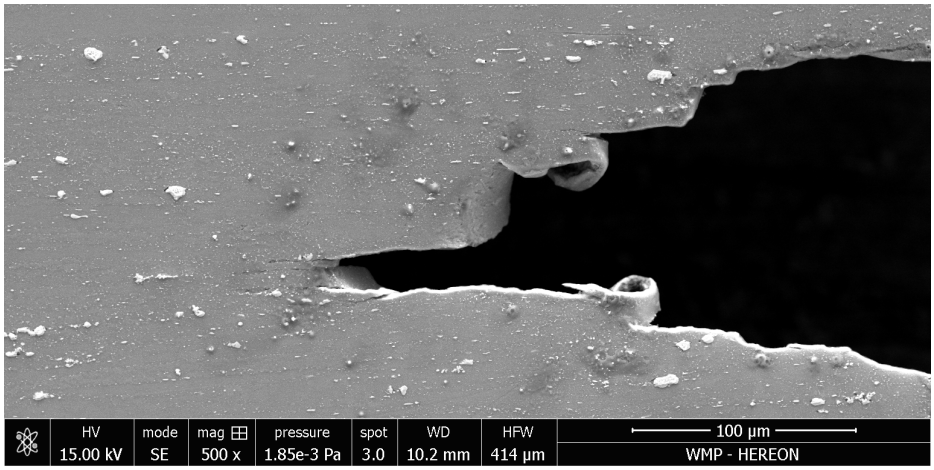

Fig. 5: Backscattered electron images of the defect tip in wire extruded from billet with 3 mm bore. Precipitate orientation and intergranular defects in extrusion direction (left to right) are visible.

Mechanical Properties. Another correlation with the change in material flow is seen in the hardness distribution in the extrudates. While for all samples the hardness over wire length slowly increases from around 80 HV at the tip to around 90 HV after 25 mm, for extrusions from billets with 6 mm bore, see Fig. 6c, additionally a pronounced hardness gradient across the wire diameter is observed. While compared to the core, the edges of the wires typically show an increase of up to 5 HV towards the end of the process, Fig. 6a and b, this difference amounts to more than 15 HV in the wires from billets with 6 mm bore.

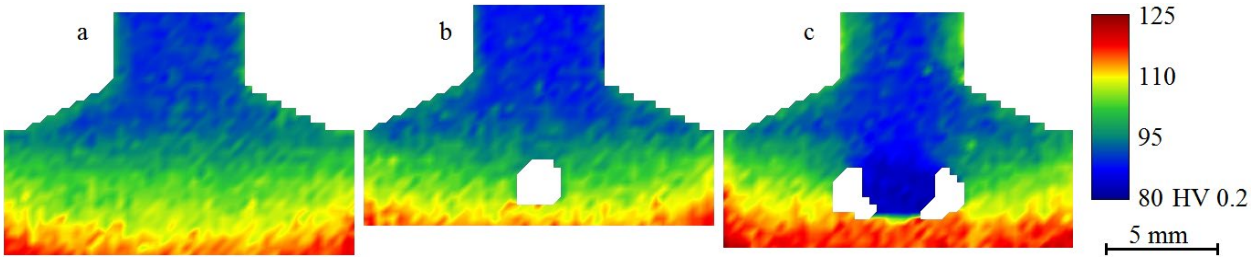

Fig. 6: Vickers micro-hardness mapping of the cross-sections through the processing zone for friction extrusions from a) solid billet, b) billets with 3 mm and c) with 6 mm bore.

The hardness distribution in the feedstock in front of the die shows overall good comparability for all billet geometries. Notable is the significantly lower hardness in the material flowing opposed to the extrusion direction in the extrusion from billets with 6 mm bore. The material filling up the drill tip cavity presents a hardness of 80 HV, comparable to the tip of the wire. Since strain and thermal history largely define the hardness for these samples exposed to otherwise identical conditions, this observation supports the hypothesis that the back-flowing material forms early on

in the friction extrusion process and moves with the plunging die into the feedstock, enabling defect free extrusion.

Conclusions

Solid wires from AA 2219 have been produced by friction extrusion. The behavior of defects through friction extrusion processing, introduced by centric bores in the feedstock, was analyzed with regard to interaction between shear introduction and material flow. Furthermore, efficiency of defect closure and contributing effects were discussed. The main findings summarize as follows:

- Removal of core material can have significant impact on material flow.
- Distinct defect closure mechanisms are observed for different dimensions of the introduced feedstock defect.
- Larger centric defects experienced faster closure and complete consolidation.
- Increased radial and especially backflow of feedstock material benefits defect closure.
- Potential approach for improving defect closure in low shear influenced process zones presented, e.g. for friction extrusion or wires from chips.

To further investigate the defect closure mechanism it is suggested to perform stop-action experiments, extend the defect size range as well as introducing off-center defects. A consequent utilization of the gained knowledge poses the extension to non-bulk feedstock e.g. chips for recycling purposes.

Funding

This project has received funding from the European Research Council (ERC) under the European Union's Horizon 2020 research and innovation programme (grant agreement No 101001567).

Data Availability

The data related to this research is available online (https://doi.org/10.5281/zenodo.10456380).

References

[1] W.M. Thomas, E.D. Nicholas and S.B. Jones, U.S. Patent 5,262,123. (1993).

[2] D. Baffari, A.P. Reynolds, A. Masnata, L. Fratini and G. Ingarao, Friction stir extrusion to recycle aluminum alloys scraps: Energy efficiency characterization, J. Manuf. Process. 43 (2019) 63-69. https://doi.org/10.1016/j.jmapro.2019.03.049

[3] W. Tang and A.P. Reynolds, Production of wires via friction extrusion of aluminum alloy machining chips, J. Mater. Process. Technol. 210(15) (2010) 2231-2237. https://doi.org/10.1016/j.jmatprotec.2010.08.010

[4] A. Hosseini Tazehkandi, E. Azarsa, B. Davoodi and Y. Ardahani, Effect of process parameters on the physical properties of wires produced by friction extrusion method, Int. J. Adv. Eng. Technol. 3 (1) (2012) 592-597.

[5] L. Rath, U. Suhuddin and B. Klusemann, Comparison of friction extrusion processing from bulk and chips of aluminum-copper alloys, Key Engineering Materials 926 (2022) 471-480. https://doi.org/10.4028/p-vw04z5

[6] M. Gelaw, P.J. Ramulu, D. Hailu and T. Desta, Manufacturing and mechanical characterization of square bar made of aluminium scraps through friction stir back extrusion process, J. Eng. Des. Technol. (2018) 16:4. https://doi.org/10.1108/JEDT-02-2018-0030

[7] R.A. Behnagh, R. Mahdavinejad, A. Yavari, M. Abdollahi and M. Narvan, Production of wire from AA7277 aluminum chips via friction-stir extrusion (FSE), Metall. Mater. Trans. B 45 (2014) 1484-1489. https://doi.org/10.1007/s11663-014-0067-2

[8] X. Li, W. Tang and A.P. Reynolds, Visualization of material flow in friction extrusion, in H. Weiland, A.D. Rollett and W.A. Cassada (Eds.), ICAA13: 13th International Conference on Aluminum Alloys, TMS (The Minerals, Metals and Materials Society), Pittsburgh, 2012, pp. 1659-1664. https://doi.org/10.1007/978-3-319-48761-8_248

[9] X. Zhao, M.A. Sutton, H. Zhang, X. Deng, A.P. Reynolds, X. Ke and H.W. Schreier, Stereo image based motion measurements in fluids: Experimental validation and application in friction extrusion, Exp. Mech. 55 (2015) 177-200. https://doi.org/10.1007/s11340-014-9907-x

[10] X. Li, W. Tang, A.P. Reynolds, W.A. Tayon and C.A. Brice, Strain and Texture in friction extrusion of aluminum wire, J. Mater. Process. Technol. 229 (2016) 191-198. https://doi.org/10.1016/j.jmatprotec.2015.09.012

[11] R.M. Halak, L. Rath, U.F.H. Suhuddin, J.F. dos Santos and B. Klusemann, Changes in processing characteristics and microstructural evolution during friction extrusion of aluminum, Int. J. Mater. Form. (2022) 15:24. https://doi.org/10.1007/s12289-022-01670-y

[12] D. Baffari, A.P. Reynolds, X. Li and L. Fratini, Influence of processing parameters and initial temper on Friction Extrusion of 2050 aluminum alloy, J. Manuf. Process. 28 (2017) 319-325. https://doi.org/10.1016/j.jmapro.2017.06.013

[13] S. Whalen, M. Olszta, C. Roach, J. Darsell, D. Graff, Md. Reza-E-Rabby, T. Roosendaal, W. Daye, T. Pelletiers, S. Mathaudhu and N. Overman, High ductility aluminum alloy made from powder by friction extrusion, Materialia 6 (2019) 100260. https://doi.org/10.1016/j.mtla.2019.100260